


ARTICLE

DOI: 10.1038/s42004-018-0066-3

OPEN

^{29}Si NMR of aqueous silicate complexes at gigapascal pressures

Corey D. Pilgrim ¹, Christopher A. Colla^{2,5}, Gerardo Ochoa¹, Jeffrey H. Walton ^{3,4} & William H. Casey ^{1,2}

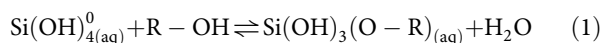
Geochemists have models to predict solute speciation and mineral equilibria in aqueous solutions up to 1200 °C and 6 GPa. These models are useful to uncover reaction pathways deep in the Earth, though experimental confirmation is extremely difficult. Here we show speciation changes among aqueous silicate complexes to pressures of 1.8 GPa through use of a high-pressure solution-state NMR probe. The radiofrequency circuit uses a microcoil geometry that is coupled with a piston-cylinder pressure cell to generate and maintain these high pressures. The 1.8 GPa pressure corresponds to pressures reached at the lower crust or upper mantle. Although these experiments are limited to ambient temperature, we show that the increased pressure affects complexation and oligomerization reactions by eliminating bulk waters and that the pressure effects are completely reversible.

¹Department of Chemistry, University of California, 1 Shields Avenue, Davis, CA 95616, USA. ²Department of Earth and Planetary Sciences, University of California, 1 Shields Avenue, Davis, CA 95616, USA. ³Nuclear Magnetic Resonance Facility, University of California, 1 Shields Avenue, Davis, CA 95616, USA. ⁴Biomedical Engineering Graduate Group, University of California, 1 Shields Avenue, Davis, CA 95616, USA. ⁵Present address: Geochemistry Department, Energy Geosciences Division, Lawrence Berkeley National Laboratory, 1 Cyclotron Road, Berkeley, CA 94720, USA. Correspondence and requests for materials should be addressed to W.H.C. (email: whcasey@ucdavis.edu)

The elucidation of aqueous silicate complexes is of particular interest to geochemists as the composition of the Earth is dominated by silicate minerals—the natural abundance of silicon in the crust is almost 29% by weight¹. Much of the chemistry that is known for inorganic silicate solutions and associated thermodynamics is based upon hydrothermal solubility experiments^{2–5}, which are often coupled with vibrational⁶, optical^{7,8}, X-ray^{9,10}, or nuclear magnetic resonance (NMR)¹¹ spectroscopies. Silicon is present in biological systems, but the role of this silicon is not fully understood^{12,13}.

In dilute, near-neutral solutions aqueous silicon generally exists as silicic acid, or $\text{Si}(\text{OH})_4^0$, which deprotonates at high pH. This monomer, depending on the alkalinity and speciation of the counterions of the system, can polymerize and form a myriad of soluble oligomeric species including the cubic octamer^{14–16}. The oligomers maintain a coordination number of four through either terminal hydroxides or oxo-bridges to other silicon atoms. In solids, very high pressures, such as are found deep in the Earth, can cause an increase in coordination number to six. Silicon in aqueous complexes usually coordinates to four oxygen molecules at ambient conditions, except when bonded to certain aromatic and sugar alcohols that cause the Si(IV) coordination to increase from four to five or even six. In particular, sugar alcohols with a *threo*-configured tetraol, such as xylitol, have been shown to complex the central Si(IV) in up to a hexacoordinated species^{17,18}, and aromatic diols, such as catechol, have also been shown to create *tris*-diolate-silicon species^{19,20}.

Each of the complexation reactions, either the oligomerization or the complexation of the silicic acid, follows a similar reaction pathway, that of a simple condensation reaction (where R can be either the $\text{Si}(\text{OH})_3$ fragment or an organic structure):¹⁴



In the case of the oligomerization of the silicic acid, this step can be repeated until, for example, the octamer species is formed (Q^3_8 , using the nomenclature of Engelhardt²¹), and ultimately solid precipitates.

Because so few silicate complexes are chromophores, NMR has become one of the most useful techniques for following speciation. This method has yielded much insight into the character of the polymeric species in solution²², and also the presence of new organic complexes in solution. ²⁹Si is the NMR active nucleus of silicon, which has a natural abundance of 4.7% and is a nucleus with medium sensitivity²³.

While the solution chemistry of silicon has been extensively studied using NMR, particularly at high pH, it has not previously been studied at gigapascal pressures. At these high pressures, the static dielectric constant of water ($\epsilon = 78$ at ambient conditions), reaches values greater than 100. This increase allows the solvent to support more ionized solutes²⁴.

In recent years, developments of high-pressure solution NMR probes yielded information about the complexation of borate species, up to 1.2 GPa in pressure^{25,26}. Efforts have also been made to increase the pressure threshold, robustness, and sensitivity of these types of probes, to the point where they can now reach 2.8 GPa^{27–29}. Furthermore, there are active efforts to increase this pressure threshold but most designs limit the sample volume to sub microliter volumes where induction NMR detection of solutes is difficult (see Supplementary note 1)^{30–33}.

Herein, we report the use of a narrow-bore high-pressure NMR solution probe coupled with a high-power shim stack that is used to explore the complexation chemistry of aqueous silicate solutions to 1.8 GPa. An image of the probe, coupled with a schematic, is included in Fig. 1. When pressure is applied to different aqueous silicate complexes, the silicate center tends to minimize

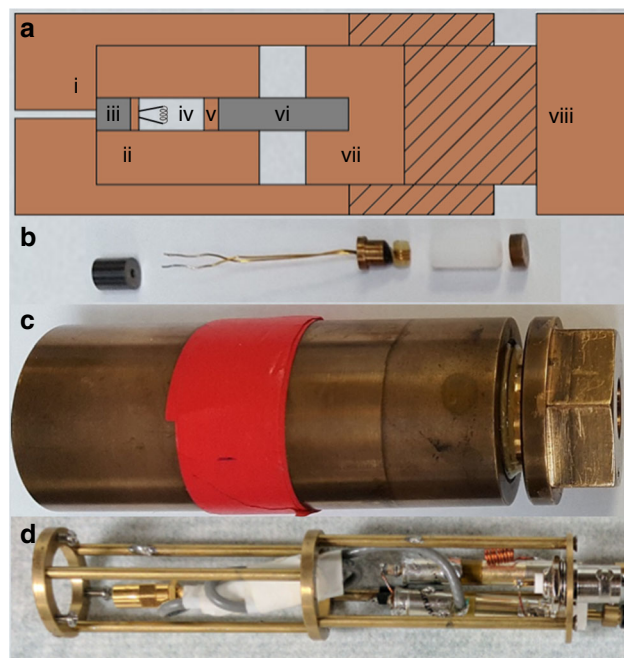


Fig. 1 The high-pressure cell and NMR circuit. **a** The schematic is of the pressure cell alone, where the labels correspond to: (i) the beryllium copper (BeCu) outer shell, (ii) the inner BeCu cylinder, (iii) a tungsten-carbide (WC) spacer, (iv) the BeCu feedthrough with RF coil and Delrin® cap, (v) the BeCu anti-extrusion disc, (vi) the WC plunger, (vii) the BeCu pressure plate, and (viii) the BeCu locknut. Pictures of the feedthrough (**b**), the pressure cell (**c**), and the NMR circuit (**d**) are shown, with the feedthrough taken apart to show detail. Scale can be gauged by the diameter of the smaller parts, which are 6.3 mm in diameter. The three-turn solenoid is 28 AWG BeCu wire

the volume of the solution by favoring complexation of water into the inner sphere of the silicon. Interestingly, the *tris*-catecholate silicate complex is such a tightly bound complex that pressure does not induce a change in the coordination environment; we detect no species as pressure is increased other than the *tris*-catechol silicate complex.

Results

Silicate oligomers. A solution containing various oligomers of Si (IV) was prepared using ²⁹Si-labeled SiO_2 , and spectra of this solution were initially collected in a high-resolution NMR spectrometer before compressing the sample. The solution contained the silicic acid monomer (Q^0), dimer (Q^1_2), cyclic trimer (Q^2_3), cyclic tetramer (Q^2_4), and prismatic hexamer (Q^3_6), consistent with assignments in the literature. The monomer, dimer, and cyclic trimer are the dominant species in this solution, which can be seen in Fig. 2a. This solution sample was placed within the high-pressure cell and subjected to a series of experiments at ambient temperature where the pressure was increased stepwise to 1.8 GPa. The sample was then returned to ambient conditions and changes in the peaks were found to be reversible.

In high-pressure NMR measurements (Fig. 2b), the monomer, dimer, and cyclic trimer are all detectable, while the cyclic tetramer and prismatic hexamer were undetectable. As pressure is increased, the signal for the cyclic trimer steadily diminishes to the point that it disappears at a nominal pressure of 0.9 GPa. The signal assigned to the dimer also diminishes relative to the monomer peak. The signals assigned to the dimer and cyclic trimer both return to their initial intensities once pressure is

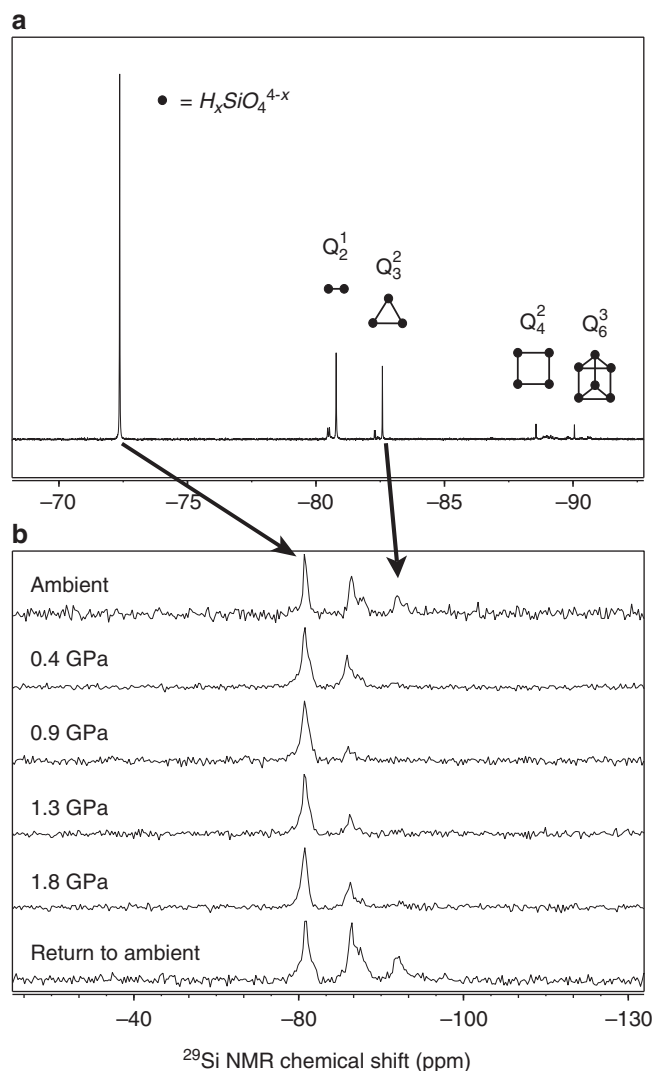


Fig. 2 ^{29}Si NMR of the silicate oligomers. **a** High-resolution ^{29}Si NMR spectrum of silicate oligomers in solution. Chemical diagrams modified from Kinrade et al.¹⁴ **b** ^{29}Si NMR in the high-pressure NMR probe, with pressures ranging from ambient conditions up to 1.8 GPa. Note a reduction in the peak intensities of both the dimer (Q_2^1) and the cyclic trimer (Q_2^3)

relieved. Uncertainties in the pressure estimates are ± 0.25 GPa, unless otherwise indicated, and were determined as the 95% prediction interval of five separate calibrations (see Supplementary Figure 1).

Sugar alcohol complexes. A solution of ^{29}Si labeled- SiO_2 was created where the five-carbon sugar alcohol, xylitol ((2R, 3R, 4S)-Pentane-1,2,3,4,5-pentol), was doped into the system, similar to the composition used by Kinrade et al.¹⁷ The NMR spectrum of this solution was first collected using a high-resolution NMR spectrometer at ambient pressures. This spectrum confirmed the presence of the four-coordinate silicic-acid species (includes both $\text{Si}(\text{OH})_4^0 + \text{SiO}(\text{OH})_3^-$) as well as both the five-coordinate and six-coordinate Si-sugar alcohol complexes (Fig. 3a). This solution was then placed within the high-pressure cell and subjected to a series of pressures, up to 1.2 GPa. Higher pressures caused freezing of the solution, but this freezing was reversible upon release of the pressure and all peaks recovered.

In the high-pressure series (Fig. 3b), the spectra show virtually no change in speciation of the silicon complexes at the lowest

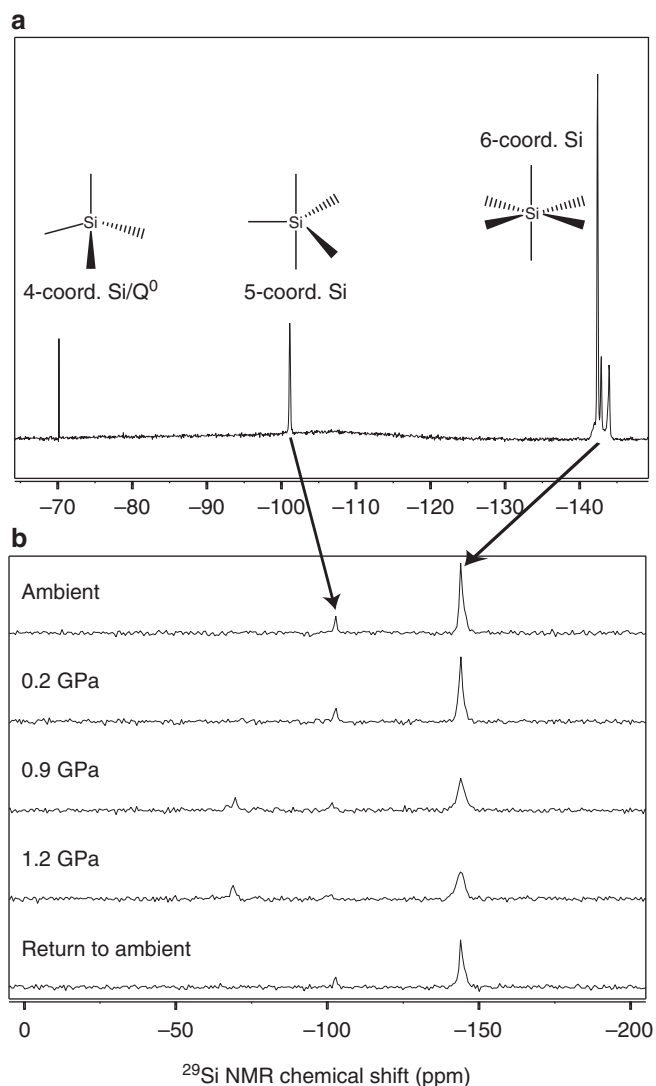


Fig. 3 ^{29}Si NMR of the silicon-xylitol complex. **a** A high-resolution ^{29}Si NMR spectrum of the xylitol-Si(IV) solution, where the four-coordinate, five-coordinate, and six-coordinate silicon species are seen in solution. **b** ^{29}Si NMR spectra of the same solution using the high-pressure NMR probe, measured up to 1.2 GPa (the solution froze immediately above this pressure). Note that the peak assignable to silicic acid appears with increased pressure and then disappears upon return to ambient conditions

pressures (up to 0.2 GPa). Only peaks assignable to the five- and six-coordinate Si(IV) complexes were apparent. The peak assigned to silicic acid, which is visible in the high-resolution NMR spectrum at ambient pressure, has an intensity below the detection limit of the high-pressure probe. However, as pressure is increased, there is a change in the relative peak intensities. The intensities of peaks assigned to the five- and six-coordinate complexes decrease with pressure, and the peak assigned to silicic acid increases up to the highest pressure of 1.2 GPa. The appearance of the peaks is reversible and the peak assigned to silicic acid once again reduces below the signal-to-noise threshold when pressure is relieved. Peak separations are constant with pressure.

Catechol complex. A third solution consisting of dissolved ^{29}Si labeled SiO_2 was formulated with catechol (1,2-dihydroxybenzene) to create the *tris*-catecholate complex. An excess of

Table 1 Solution compositions of the analyzed samples

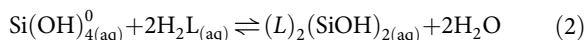
Solution	SiO ₂ (mol)	NaOH (mol)	Xylitol (mol)	Catechol (mol)	Ratio of Analytes (Si:OH:Organic)
1	0.00060	0.00182	–	–	1.0: 3.0: 0.0
2	0.00085	0.00216	0.00624	–	1.0: 2.5: 7.3
3	0.00064	0.00183	–	0.00273	1.0: 2.9: 4.2

All solutions were made in 2 mL of isotopically enriched D₂O

catechol was used (Table 1). In this spectrum, a single peak was seen at –145 ppm (externally referenced to the silicic acid at –71 ppm), which provides good agreement with the listed chemical shift of –146 ppm found in Evans et al.³⁴ The peak due to the *tris*-catecholate also happens to reside within the same chemical shift region as the six-coordinate sugar alcohols seen previously, consistent with the assignment of hexacoordinated Si(IV). This spectrum is shown as Fig. 4a.

This solution was then placed within the high-pressure cell and compressed, where the maximum pressure reached was 1.5 GPa. The ²⁹Si NMR pressure series can be seen in Fig. 4b. At this pressure, the peak due to the *tris*-catecholate broadened, which experience has shown commonly indicates that the solution is close to freezing—as the viscosity of the solution increases, the correlation time τ_c decreases, which causes broadening of the peak³⁵. When the solution was returned to ambient pressures, the initial peak shape returned.

Chemical interpretation. The pressure-induced speciation changes presented in Figs. 2 and 3 can be understood by following the movement of water between the bulk solution and the silicon species in the reaction. Generally, increases in the coordination numbers of the Si(IV)-sugar complexes are associated with release of water to the bulk solvent. Conversely, these larger silicate oligomers are then reduced to smaller species as bulk waters are packed back into the inner-coordination-sphere of Si(IV) as pressure is increased. Consider as an example the formation of a *bis*-diolato-hydroxo-structure with Si(IV) resulting in a Si(IV) coordinated by four *oxo* atoms from the two diolate anion and two hydroxides. This hypothetical six-coordinated Si(IV) is portrayed as: (L)₂(SiOH)₂, where L represents the diolate anion ([–]O–R–R–O[–]):



The trend toward smaller complexes with increased pressure is the reverse of this condensation reaction, and is consistent with results presented in Figs. 2 and 3. The volume change due to the elimination of a bulk water molecule during hydrolysis is negative and drives this trend towards a reduction in Si(IV) coordination number. Water molecules are packed more efficiently into coordination sphere of Si(IV) than in bulk solution. Thus the change in volume to eliminate a bulk water ($V^\circ \sim -18 \text{ cm}^3 \text{ mol}^{-1}$) by packing it around Si(IV) overwhelms any increase in volume from elimination and solvation of the ligand.

Next, consider the last set of experiments involving the catecholate-Si(IV) complex. The hypothesis motivating these experiments is that pressure would favor *bis*-catecholate or *mono*-catecholate species as these would pack water more effectively

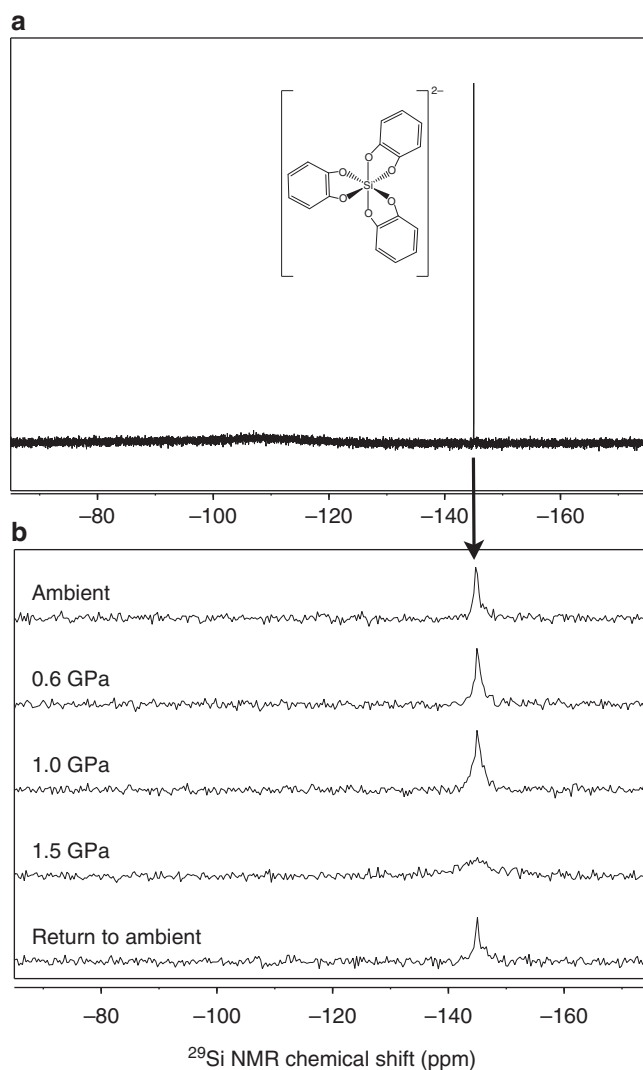
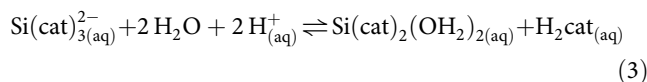


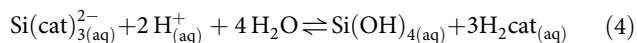
Fig. 4 ²⁹Si NMR of the *tris*-catecholate silicon complex. **a** A high-resolution ²⁹Si NMR spectrum of the *tris*-catecholate-Si(IV) complex. **b** ²⁹Si NMR spectra of the same solution using the high-pressure NMR probe, measured up to 1.5 GPa, where the solution was near freezing. Note that changes in the spectrum with pressure are reversible

than the bulk solvent and be favored at pressure:



Note that the coordination number of six around Si(IV) is preserved by the ligand-exchange reaction and such a *bis*-catecholate complex has been crystallized by Hahn et al.³⁶

However, our experiments show this hypothesis to be refuted, at least at slightly excessive catechol concentrations—there are no aqueous hexacoordinated catecholate complexes of ^{29}Si evident save for the familiar *tris*-catecholate complex. If some of the *oxo* ligands bridging to Si(IV) from the catecholate were converted to bridging *hydroxo* ligands, the number of protons and waters in reaction (3) would change, but not the general trend. Similarly, a competing reaction that reduces the coordination number of Si(IV), while still heavily favored by increases in pressure, would cause silica precipitation:



If this were to occur, the solubility of $\text{SiO}_2(\text{s})$ is less than $\sim 10^{-3}$ molal at ambient conditions and near-neutral pH, so destruction of the *tris*-catecholate-Si(IV) complex by pressure would lead to diminished ^{29}Si signals, which we do not observe in the high-pressure NMR spectra. Instead we observe a clear constant signal that is assignable to the *tris*-catecholate-Si(IV) complex alone.

Of course, the reaction volume for these Si(IV)-complexation reactions reflects all changes in solvation, including solvation of the released ligands. However, the data described above consistently indicate that dominant term is the uptake or release of bulk waters by the condensation reaction (1), above. (Calculations to identify reasonable stoichiometries based upon energetics are included in the Supplementary Table 1 and visualized in Supplementary Figure 2.)

Discussion

High-pressure ^{29}Si NMR data indicate that the condensation reactions that lead to the complexation of aqueous silicate are reversed at elevated pressure. At pressures greater than a GPa, it seems that silicate speciation is determined by forming aqueous complexes that pack water more efficiently. These pressures correspond to a column of water reaching to the deepest part of the Earth's crust; the NMR data were not, however, collected at the elevated temperatures of this region but such design changes are underway. In these regions, reactions between mobile fluids and silicate minerals redistribute mass and alter mineralogical composition. While the reactions of silicon deep in the Earth's crust are done at hydrothermal temperatures, the ambient data presented herein suggest that much of the pressure-induced speciation change is attributable to simple transfer of waters into, and out of, the inner-coordination spheres of Si(IV).

Methods

High-pressure NMR. The high-pressure NMR probe uses a beryllium copper body (BeCu) with a tungsten carbide (WC) plunger and spacer combination to allow for pressures up above 2.0 GPa. The diameter of the probe is 39 mm and is designed for a narrow-bore magnet system. The circuit is an LC-circuit coupled with a three-turn microcoil made of 28-AWG BeCu wire, where the tuning and match capacitors can be exchanged depending on the nuclei studied. The quality factor of the circuit at 79.48 MHz is $Q = 23.7$.

The aqueous sample is held within a small portion of PEEK tubing, which is glued in place within the microcoil. The coil is immersed in fluorocarbon oil (Halocarbon 6.3) as the pressure transmission fluid and the probe is assembled as in Fig. 1. A hydraulic press is used to apply pressure to the sample while a lock-nut is screwed in place to lock in pressure. The gauge pressure of the press has been calibrated to the internal pressure of the sample via the technique of ruby fluorescence, measured from a spherical ruby within the sample cell (See Supplementary Methods). This ruby is coupled to a fiber-optic cable and the fluorescence is measured via an external optical spectrometer³⁷.

The high-powered shim stack was designed by Resonance Research, Inc., and is designed for use inside a wide-bore superconducting magnet. The water-cooled shim coils have been specifically designed to provide higher power (up to 5 Amps per channel) for shimming this probe. The channels available are Z^0 , X , Y , Z , Z^2 , Z^3 , X^2-Y^2 , and $2XY$. The probe is tuned down to ^2H ($\omega_{\text{RF}} = 61.40$ MHz at 9.4 T) and shimmed using the D_2O peak in all samples. All high-pressure measurements were carried out using a wide-bore Oxford superconducting magnet (9.4 T)

coupled to a Bruker DRX console. ^{29}Si ($\omega_{\text{RF}} = 79.47$ MHz at 9.4 T) measurements for all three samples used a single-pulse $^{\text{zgpg}}$ experiment with a smaller RF tip-angle³⁸. The peaks in the high-pressure spectra were referenced using the high-resolution spectra, with the Q^0 peak set at -71 ppm. High-resolution spectra were measured using a Bruker DRX500 system (11.75 T) using a 5 mm PABBO broadband probe. Typical quality factors for the resonance circuit are ~ 20 , but can of course fluctuate as each experiment is run with a different coil assembly.

Details for each experiment are: (i) ^{29}Si oligomer solution: A 30° Ernst angle was used to create a pulse length of $3.6 \mu\text{s}$ at 34 W in power (3.5 dB using a Bruker BLAX300 amplifier). The smaller tip angle was used to reduce the acquisition time per scan as the longest measured T_1 was 6.6 s. Total acquisition time per scan (AQ + D1) was 1.0 s, and 50,000 transients were measured, resulting in ~ 14 h experiments. (ii) ^{29}Si sugar alcohol (xylitol) solution: A 30° Ernst angle was used to create a pulse length of $4.8 \mu\text{s}$ at 34 W in power (3.5 dB using a Bruker BLAX300 amplifier). The smaller tip angle was used to reduce the acquisition time per scan as the longest measured T_1 was 7.0 s. Total acquisition time per scan (AQ + D1) was 1.0 s, and 30,000 transients were measured, resulting in ~ 8 h experiments. (iii) ^{29}Si catecholate solution: A 15° Ernst angle was used to create a pulse length of $2.0 \mu\text{s}$ at 34 W in power (3.5 dB using a Bruker BLAX300 amplifier). The smaller tip angle was used to reduce the acquisition time per scan as the T_1 of the catecholate complex was 60.6 s. Total acquisition time per scan (AQ + D1) was 2.1 s, and 26,000 transients were measured, resulting in ~ 16 h experiments.

Solution Preparation. The three silicate solutions were made using 98.7% isotopically enriched SiO_2 (Isoflex, USA) digested in NaOH and D_2O using a Teflon-lined stainless-steel Parr reactor vessel at 80°C for 12 h. The resulting solutions were clear and free of colloids. For the solution containing only silicate oligomers (Solution 1), nothing more was added. For solutions 2 and 3, xylitol and catechol were added after the solution was allowed to cool to room temperature. No other adulteration was done to the solutions. The exact solution composition is included in Table 1. The resulting solutions were stable for weeks with no sign of gelling. The solution containing catechol was made under an inert argon atmosphere, where the initial solution had a slight rose tint. However, the solution began to darken slowly, even after sealing the sample in the argon environment, covering with foil, and placing in the refrigerator. Initial high-resolution ^{29}Si NMR was run on the fresh solution and eventually compared to the NMR of the dark brown solution—no difference between the two spectra was seen.

Data availability

The authors declare that the data supporting the findings of this study are available from the corresponding author on reasonable request.

Received: 26 May 2018 Accepted: 3 October 2018

Published online: 23 October 2018

References

- Rudnick, R. L. & Gao, S. in *Treatise on Geochemistry* (Holland, H. D. & Turekian, K. K. eds.) 1–51 (Elsevier, Amsterdam, 2014).
- Manning, C. E. The solubility of quartz in H_2O in the lower crust and upper mantle. *Geochim. Cosmochim. Acta* **58**, 4831–4839 (1994).
- Newton, R. C. & Manning, C. E. Quartz solubility in H_2O -NaCl and H_2O - CO_2 solutions at deep crust-upper mantle pressures and temperatures: 25 kbar and 500°C . *Geochim. Cosmochim. Acta* **64**, 2993–3005 (2000).
- Hunt, J. D. & Manning, C. E. A thermodynamic model for the system near the upper critical end point based on quartz solubility experiments at 500°C and 50 kbar. *Geochim. Cosmochim. Acta* **86**, 196–213 (2012).
- Seward, T. M. Determination of the first ionization constant of silicic acid from quartz solubility in borate buffer solutions to 350°C . *Geochim. Cosmochim. Acta* **38**, 1651–1664 (1974).
- Facq, S., Daniel, I., Montagnac, G., Cardon, H. & Sverjensky, D. A. Carbon speciation in saline solutions in equilibrium with aragonite at high pressure. *Chem. Geol.* **431**, 44–53 (2016).
- Liu, W., Migdisov, A. & Williams-Jones, A. The stability of aqueous nickel(II) chloride complexes in hydrothermal solutions: Results of UV-Visible spectroscopic experiments. *Geochim. Cosmochim. Acta* **94**, 276–290 (2012).
- Migdisov, A. A., Zevin, D. & Williams-Jones, A. E. An experimental study of Cobalt (II) complexation in Cl^- and H_2S -bearing hydrothermal solutions. *Geochim. Cosmochim. Acta* **75**, 4065–4079 (2011).
- Pokrovski, G. S. et al. Sulfur radical species form gold deposits on Earth. *Proc Natl Acad. Sci. USA* **112**, 13484–13489 (2015).
- Tooth, B. et al. Bismuth speciation in hydrothermal fluids: an X-ray absorption spectroscopy and solubility study. *Geochim. Cosmochim. Acta* **101**, 156–172 (2013).
- Swaddle, T. W., Salerno, J. & Tregloan, P. A. Aqueous aluminates, silicates, and aluminosilicates. *Chem. Soc. Rev.* **23**, 319 (1994).

12. Candy, J. M. et al. Aluminosilicates and senile plaque formation in Alzheimer's Disease. *Lancet* **327**, 354–356 (1986).
13. Exley, C. Silicon in life: a bioinorganic solution to bioorganic essentiality. *J. Inorg. Biochem.* **69**, 139–144 (1998).
14. Kinrade, S. D. & Swaddle, T. W. Silicon-29 NMR studies of aqueous silicate solutions. 2. Transverse ^{29}Si relaxation and the kinetics and mechanism of silicate polymerization. *Inorg. Chem.* **27**, 4259–4264 (1988).
15. Lippmaa, E. T., Alla, M. A., Pehk, T. J. & Engelhardt, G. Solid-state high resolution NMR spectroscopy of spin 1/2 nuclei (^{13}C , ^{29}Si , ^{119}Sn) in organic compounds. *J. Am. Chem. Soc.* **100**, 1929–1931 (1978).
16. Sjöberg, S., Öhman, L.-O. & Ingri, N. Equilibrium and structural studies of silicon(IV) and aluminium(III) in aqueous solution. 11. Polysilicate formation in alkaline aqueous solution. A combined potentiometric and ^{29}Si NMR study. *Acta Chem. Scand.* **39A**, 93–107 (1985).
17. Kinrade, S. D. et al. Stable five- and six-coordinated silicate anions in aqueous solution. *Science* **285**, 1542–1545 (1999).
18. Benner, K., Klüfers, P. & Vogt, M. Hydrogen-bonded sugar-alcohol trimers as hexadentate silicon chelators in aqueous solution. *Angew. Chem. Int. Ed.* **42**, 1058–1062 (2003).
19. Barnum, D. W. Catechol complexes with silicon. *Inorg. Chem.* **9**, 1942–1943 (1970).
20. Sjöberg, S., Ingri, N., Nenner, A. & Öhman, L.-O. Equilibrium and structural studies of silicon(IV) and aluminium(III) in aqueous solution. 12. A potentiometric and ^{29}Si -NMR study of silicon tropolonates. *J. Inorg. Biochem.* **24**, 267–277 (1985).
21. Engelhardt, G., Jancke, H., Hoebbel, D. & Wieker, W. Strukturuntersuchungen an Silicatanionen in wässriger Lösung mit Hilfe der ^{29}Si -NMR-Spektroskopie. *Chem. Inf.* **5**, 109–110 (1974).
22. Harris, R. K. & Newman, R. H. ^{29}Si NMR studies of aqueous silicate solutions. *J. Chem. Soc. Faraday Trans. 2* **73**, 1204 (1977).
23. Uhlig, F. in *Organosilicon Compounds*, 59–77 (Academic Press, Amsterdam, 2017).
24. Fernández, D. P., Mulev, Y., Goodwin, A. R. H. & Sengers, J. M. H. L. A database for the static dielectric constant of water and steam. *J. Phys. Chem. Ref. Data* **24**, 33–70 (1995).
25. Pautler, B. G. et al. A high-pressure NMR probe for aqueous geochemistry. *Angew. Chem. Int. Ed.* **53**, 9788–9791 (2014).
26. Edwards, T., Endo, T., Walton, J. H. & Sen, S. Observation of the transition state for pressure-induced $\text{BO}_3 \rightarrow \text{BO}_4$ conversion in glass. *Science* **345**, 1027–1029 (2014).
27. Ochoa, G. et al. ^2H and ^{139}La NMR spectroscopy in aqueous solutions at geochemical pressures. *Angew. Chem. Int. Ed.* **54**, 15444–15447 (2015).
28. Ochoa, G., Colla, C. A., Klavins, P., Augustine, M. P. & Casey, W. H. NMR spectroscopy of some electrolyte solutions to 1.9GPa. *Geochim. Cosmochim. Acta* **193**, 66–74 (2016).
29. Augustine, M. P., Ochoa, G. & Casey, W. H. Steps to achieving high-resolution NMR spectroscopy on solutions at GPa pressure. *Am. J. Sci.* **317**, 846–860 (2017).
30. Meier, T., Reichardt, S. & Haase, J. High-sensitivity NMR beyond 200,000 atmospheres of pressure. *J. Magn. Reson.* **257**, 39–44 (2015).
31. Meier, T. et al. Magnetic flux tailoring through Lenz lenses for ultrasmall samples: a new pathway to high-pressure nuclear magnetic resonance. *Sci. Adv.* **3**, 1–9 (2017).
32. Meier, T. in *Annual Reports on NMR Spectroscopy* 93 (G. A. Webb, ed.) 1–74, (Academic Press, Amsterdam, 2018).
33. Aslam, N. et al. Nanoscale nuclear magnetic resonance with chemical resolution. *Science* **357**, 67–71 (2017).
34. Evans, D. F., Parr, J. & Coker, E. N. Nuclear magnetic resonance studies of silicon(IV) complexes in aqueous solution-I. Tris-catecholato complexes. *Polyhedron* **9**, 813–823 (1990).
35. Harris, R. K. *Nuclear Magnetic Resonance Spectroscopy*. (Wiley, 1989)
36. Hahn, F. E., Keck, M. & Raymond, K. N. Catecholate complexes of silicon: synthesis and molecular and crystal structures of $[\text{Si}(\text{cat})_2]\cdot 2\text{THF}$ and $\text{Li}_2[\text{Si}(\text{cat})_3]\cdot 3.5\text{dme}$ (cat=catecholate dianion). *Inorg. Chem.* **34**, 1402–1407 (1995).
37. Mao, H. K., Xu, J. & Bell, P. M. Calibration of the ruby pressure gauge to 800 kbar under quasi-hydrostatic conditions. *J. Geophys. Res.* **91**, 4673–4676 (1986).
38. Ernst, R. R. & Anderson, W. A. Application of Fourier transform spectroscopy to magnetic resonance. *Rev. Sci. Instrum.* **37**, 93–102 (1966).

Acknowledgements

This work is supported by the U.S. Department of Energy Office of Basic Energy Sciences via grant DE-FG0205ER15693 to W.H.C. Peter Klavins is thanked for his advice about high-pressure experimentation, and Brian Devine for help with machining.

Author contributions

W.H.C., C.D.P., and C.A.C. conceived and designed the study. J.H.W. helped to design and install the high-powered shim stack and power supply. C.D.P., C.A.C., and G.O. performed the experiments. W.H.C., C.D.P., and C.A.C. wrote the manuscript.

Additional information

Supplementary information accompanies this paper at <https://doi.org/10.1038/s42004-018-0066-3>.

Competing interests: The authors declare no competing interests.

Reprints and permission information is available online at <http://npg.nature.com/reprintsandpermissions/>

Publisher's note: Springer Nature remains neutral with regard to jurisdictional claims in published maps and institutional affiliations.



Open Access This article is licensed under a Creative Commons Attribution 4.0 International License, which permits use, sharing, adaptation, distribution and reproduction in any medium or format, as long as you give appropriate credit to the original author(s) and the source, provide a link to the Creative Commons license, and indicate if changes were made. The images or other third party material in this article are included in the article's Creative Commons license, unless indicated otherwise in a credit line to the material. If material is not included in the article's Creative Commons license and your intended use is not permitted by statutory regulation or exceeds the permitted use, you will need to obtain permission directly from the copyright holder. To view a copy of this license, visit <http://creativecommons.org/licenses/by/4.0/>.

© The Author(s) 2018